

Transparent Thin-Film Transistors Using ZnMgO as Dielectrics and Channel

Huizhen Wu, Jun Liang, Guofen Jin, Yanfeng Lao, and Tiansing Xu

Abstract—An enhancement-mode ZnMgO transparent thin-film transistor (TFT) is fabricated, in which cubic-phase ZnMgO (C-ZnMgO) is used as gate insulator and hexagonal-phase ZnMgO (H-ZnMgO) is used as channel. The multilayers of C-ZnMgO and H-ZnMgO are grown on patterned indium-tin-oxide-coated glass in successive fashion at low temperature. Capacitor–voltage characteristics measured across the gate show that the H-ZnMgO channel is n-type. The C-ZnMgO isolating layer demonstrates low leakage current characteristics, i.e., 4×10^{-7} A/cm², at a bias of 10 V. The transparent TFTs display a typical channel mobility of $1.5 \text{ cm}^2 \text{ V}^{-1} \text{ s}^{-1}$ and an on/off ratio of 10^4 .

Index Terms—High- κ gate dielectrics, transparent thin-film transistors (TFTs), ZnMgO.

I. INTRODUCTION

THIN-FILM transistors (TFTs) made of amorphous silicon channel and amorphous silicon nitride (SiN_x) gate insulator have been widely used in various applications, such as organic light-emitting displays [1], [2], liquid crystal displays [3], and sensors [4]. The band gap of amorphous silicon is in the visible region (1.7 eV), and opaque metal shadow masks are integrated so that the channels are blind from visible light irradiation to prevent the generation of photon-excited carriers [5]. Undoped hexagonal ZnO is an n-type II–VI compound semiconductor, which has been used as channel layers in transparent TFTs. In TFT devices, it is preferred to use an enhancement mode in which conductivity is controlled by an applied gate voltage. However, ZnO usually has high carrier concentrations ($\sim 10^{20} \text{ cm}^{-3}$) due to intrinsic oxygen vacancies in the epitaxial layers and is difficult to low down. It is known that the carrier concentration in a semiconductor material can be changed by tuning the width of band gap, i.e., $n_i \propto \exp(-E_g/2k_0T)$. ZnO can be alloyed with MgO and realized the tailoring of the band gap, as recently demonstrated by Ohtomo *et al.* [6] and Bhattacharya *et al.* [7], with $E_g(\text{Zn}_{1-x}\text{Mg}_x\text{O}) = 3.32 + 2.0 \times (\text{Mg content})$, where E_g is the band-gap energy. ZnMgO alloy thin films have been synthesized at low growth temperatures that are compatible with various substrates, including silicon and glass.

Another key issue for ZnO TFTs is the selection of gate insulators. Various dielectric materials have been tested for ZnO-based TFTs, such as SiO₂ [8], HfO₂ [9], PbZrTiO [10], and Y₂O₃ [11], which were used as gate dielectrics. As the ZnO channel and gate dielectric are commonly of different material systems, contamination problems may arise if the two different material systems are deposited in a same growth chamber. Also, the density of dangling bonds at the interface between channel and dielectric layers could be high because of the bonding of different materials; thus, the interface may deteriorate. Further, the active channel and gate dielectric layers of TFTs are conventionally deposited in two different vacuum systems. Thus, after the growth of the channel, the sample needs to be downloaded from the vacuum system for the channel growth and be uploaded to another vacuum system for the sequential deposition of the gate dielectric. The exposure to air should contaminate channel surface and deteriorate the TFT device performance. Masuda *et al.* [8] reported that depositing ZnO onto SiO₂ degraded the isolating property of the SiO₂ layer. A 250-nm SiO₂ gate layer displayed a leakage current density of higher than 10^{-4} A/cm², although the leakage current through a 250-nm-thick SiO₂ layer (on which a ZnO layer was not deposited) was about 10^{-10} A/cm². Thus, a double-layer gate insulator (SiO₂ + SiN_x) was used to suppress the leakage current [8].

As reported by Chen *et al.* [12], the alloying of ZnO and MgO with Mg composition higher than 50% (Zn_{1-x}Mg_xO, $x > 0.5$) led to the formation of a cubic-phase ZnMgO (C-ZnMgO) crystal structure. We previously reported the application of C-ZnMgO as a high- κ dielectric material to metal–insulator–semiconductor devices [13]. Optical and electrical properties, including wide band gap ($E_g > 5.0$ eV) and higher dielectric constant ($\epsilon \sim 10.5$), were obtained. In this paper, C-ZnMgO used as an isolating gate layer and hexagonal-phase ZnMgO (H-ZnMgO) used as an active channel layer for TFT devices were successively deposited in a single deposition chamber on patterned indium-tin-oxide (ITO)-coated glass. Transparent TFTs have been fabricated.

II. EXPERIMENTAL

The substrates used for the TFT device fabrication were ITO-coated glass. Prepatterned ITO pads serve as the source and drain regions. An H-ZnMgO film was employed as the active channel between the two ITO pads, and a C-ZnMgO film was directly deposited on the H-ZnMgO film as the gate dielectric. The H-ZnMgO and C-ZnMgO film stacks were deposited on the prepatterned ITO substrate in successive fashion in the same

Manuscript received April 16, 2007. This work was supported in part by the Natural Science Foundation of China under Grant 60676003, by the National Basic Research Program of China under Grant 2006CB04906, and by the Natural Science Foundation of Zhejiang Province under Grant Z406092. The review of this paper was arranged by Editor H.-S. Tae.

H. Wu, G. Jin, and T. Xu are with the Department of Physics, Zhejiang University, Hangzhou 310027, China (e-mail: hzwu@zju.edu.cn).

J. Liang and Y. Lao are with the State Key Laboratory of Functional Materials for Informatics, Shanghai Institute of Microsystem and Information Technology, Chinese Academy of Sciences, Shanghai 200050, China.

Digital Object Identifier 10.1109/TED.2007.907126

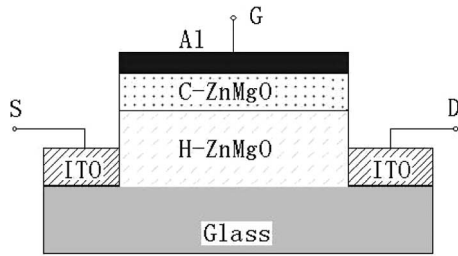


Fig. 1. Schematic cross-sectional view of the C-ZnMgO/H-ZnMgO stack TFT.

chamber of our reactive electron beam (e-beam) evaporation system [14]. Ceramic ZnMgO targets with a purity of 99.99% were used as the source materials. A $\text{Zn}_{0.99}\text{Mg}_{0.01}\text{O}$ target was used to deposit the H-ZnMgO channel, and a $\text{Zn}_{0.88}\text{Mg}_{0.12}\text{O}$ target was used to deposit the C-ZnMgO gate dielectric. It is known that the Mg content in the deposited ZnMgO film is much higher than that in the targets. The deposition of the ZnMgO thin films was carried out in an oxidizing ambience with a chamber pressure of 2×10^{-4} torr. The substrate temperature for the growth of the ZnMgO films was low, i.e., 250 °C. After deposition, the H-ZnMgO and C-ZnMgO films were annealed *in situ* at 400 °C for 1 h.

The thicknesses of the channel and gate oxide layers were 70 and 200 nm, respectively. A 200-nm Al film was deposited by e-beam evaporation for the gate electrode. The source and drain regions were then exposed by standard photolithography and wet etching of the Al layer and the two successive ZnMgO layers that were deposited on ITO pads. A 100% concentration H_3PO_4 etchant was used to expose the source/drain contacts for electrical characterization. Therefore, the gate electrode was Al, and the source and drain electrodes were ITO. The channel length and channel width were 30 and 90 μm , respectively. The TFT structure is shown in Fig. 1. Capacitance–voltage (C – V) characteristics were measured at 1 MHz by an HP 4280A impedance analyzer. Current–voltage (I – V) characteristics were measured at room temperature using an HP 4156A semiconductor parameter analyzer. Optical transmission and absorption band edge were measured by a Varian Cary 500 Scan UV spectrophotometer.

III. RESULTS AND DISCUSSION

The optical band gap E_g of the cubic-phase $\text{Zn}_{1-x}\text{Mg}_x\text{O}$ (C-ZnMgO) ($x \sim 0.6$) film is estimated to be 5.6 eV from the transmittance spectra, as shown in Fig. 2 [15], [16]. The film is optically transparent in a wide region from ultraviolet to infrared ($\lambda = 220$ –2500 nm), and the optical transmittance is about 90% in the visible region. The measured dielectric constant for the C-ZnMgO is 10.5. Hexagonal-phase $\text{Zn}_{1-y}\text{Mg}_y\text{O}$ semiconductor ($y \sim 0.14$) with an optical band gap of 3.59 eV is used as an active channel layer. The inset in Fig. 2 shows X-ray diffraction patterns of the single C-ZnMgO film and the H-ZnMgO and C-ZnMgO stacks deposited on glass substrates. The single C-ZnMgO film displays a unique (002) diffraction peak, whereas the H-ZnMgO and C-ZnMgO stacks show two diffraction peaks of (0002)-oriented hexagonal crystal and (002)-oriented cubic crystal.

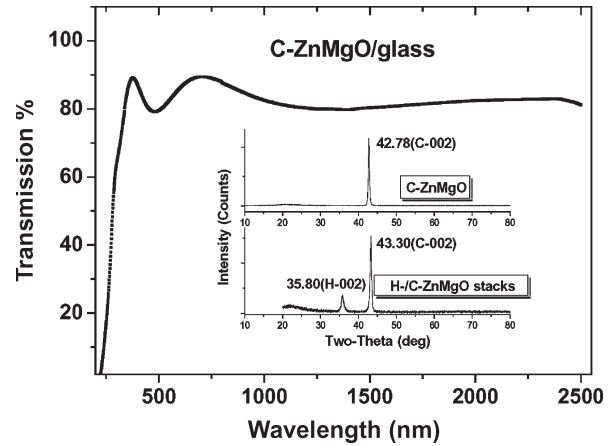


Fig. 2. Optical transmission spectra of TFT material showing that the TFT is transparent in the visible region. Inset: Plots of X-ray diffraction of C-ZnMgO and H-ZnMgO and C-ZnMgO stacks grown on glass.

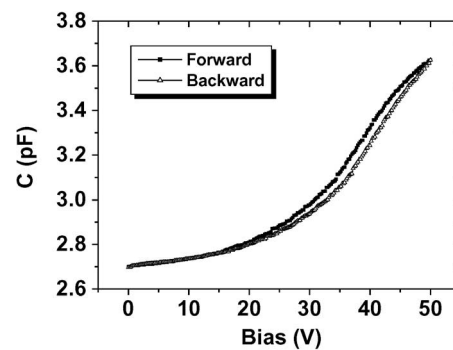


Fig. 3. C – V characteristics of C-ZnMgO/n-type H-ZnMgO/ITO structure.

The C – V characteristics of the gate-metal Al/C-ZnMgO/H-ZnMgO/ITO structure were shown in Fig. 3. The polarity of the accumulation capacitance indicates that the semiconducting oxide (H-ZnMgO) is of n-type behavior, although doping with acceptors considerably reduces the carrier density. Rare interdiffusion between the C-ZnMgO gate insulator and the H-ZnMgO active channel can be expected, as the ZnMgO stacks were successively deposited at a low temperature of 250 °C. Our previous Auger depth profile characterization showed that Mg were very stable in the ZnMgO alloy up to a high temperature of 750 °C [17]. From the C – V curve, the carrier concentration is estimated to be $2 \times 10^{17}/\text{cm}^3$. A clockwise hysteresis was observed in the C – V measurement for the devices employing C-ZnMgO as the gate oxide, indicating the presence of positive mobile ions in the C-ZnMgO film.

With the positive voltage polarity, the C – V curve shifts to the right and is saturated, indicating a negative fixed charge accumulation in the dielectric oxide near the gate dielectric/active channel interface, to which the source of fixed charges is thought to originate from the bonding of the atoms in the C-ZnMgO gate dielectric material. It differs from the interfacial characteristics of positive fixed charges between C-ZnMgO and Si [17]. Obviously, the negative fixed charges have a reverse effect on the accumulation of electrons at the interface because the negative fixed charges in the C-ZnMgO layer induce positive charges on the surface of the H-ZnMgO semiconductor

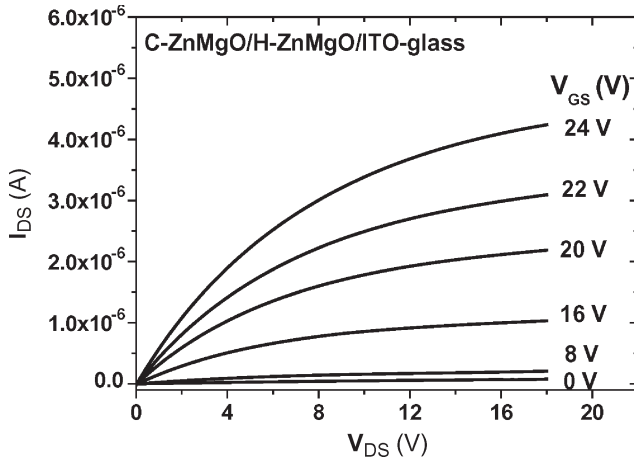


Fig. 4. I_{DS} – V_{DS} characteristics of C-ZnMgO/H-ZnMgO stack TFT with a channel length of $30\ \mu\text{m}$ and a channel width of $90\ \mu\text{m}$.

channel. As reflected from the shift of C – V curve, to realize the accumulation of electrons on the interface, a high positive voltage bias needs to be applied. The induction of positive charges on the surface also leads to the carrier scattering in the channel and the low down of mobility when TFT works. The fixed charge density D_{fc} can be estimated as follows:

$$D_{fc} = \frac{C_i}{A \cdot q} V_{FB} \quad (1)$$

where C_i is the capacitance of the oxide layer capacitor, A is the area of the capacitor, and V_{FB} is the gate flatband voltage (estimated to be $36\ \text{V}$). Therefore, the fixed charge density is estimated to be high ($\sim 1.0 \times 10^{13}/\text{cm}^2$). Strictly speaking, (1) is valid only if the semiconductor channel and the gate metal have the same work function; otherwise, the work-function difference must be considered. However, in these devices, the flatband voltage is very large that the work-function difference can be ignored.

Fig. 4 shows the drain current–drain voltage (I_{DS} – V_{DS}) characteristics measured at room temperature for the ZnMgO TFT. The modulation of the H-ZnMgO channel conductance indicates that the operation of the device is an n-channel enhancement mode, as there is a small drain current at a gate voltage of $0\ \text{V}$. Note that the leakage current is relatively low through the C-ZnMgO gate dielectric, yielding a zero intercept of I – V curves taken. Current saturation and pinch off are clearly observed, indicating that the entire channel region can be depleted of electrons. These characteristics are useful for circuit applications that employ these devices.

The drain currents I_{DS} were measured as a function of gate voltages V_{GS} at a fixed drain voltage of $10\ \text{V}$, as shown in Fig. 5. The field-effect mobility can be determined as follows [11]:

$$I_D = \frac{W}{L} \mu_{FE} C_{ox} \left[(V_{GS} - V_T) V_{DS} - \frac{V_{DS}^2}{2} \right] \quad (2)$$

where W is the channel width, L is the channel length, C_{ox} is the capacitance of gate oxide, V_T is the threshold voltage (here, $V_T \sim 16\ \text{V}$), and μ_{FE} is the field-effect mobility. Taking $V_{DS} = 10\ \text{V}$ and $V_{GS} = 20\ \text{V}$, the extracted field-

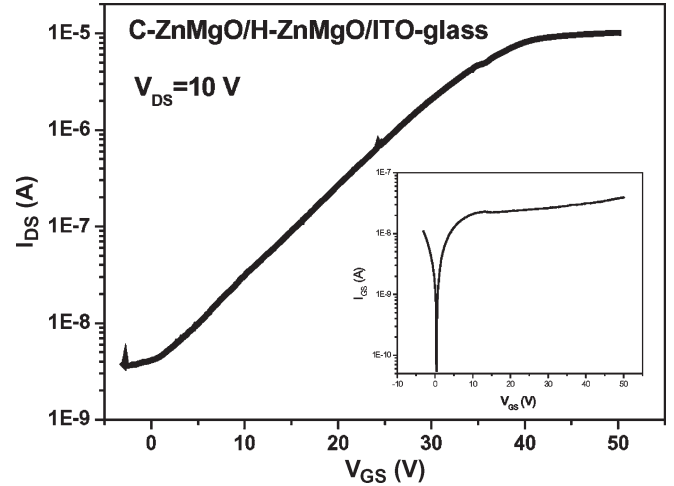


Fig. 5. Transfer characteristics of C-ZnMgO/H-ZnMgO stack TFT measured at a drain voltage of $10\ \text{V}$.

effect mobility μ_{FE} is $1.5\ \text{cm}^2\ \text{V}^{-1}\ \text{s}^{-1}$, which is higher than that of TFT composed of amorphous silicon channel ($\sim 0.5\ \text{cm}^2\ \text{V}^{-1}\ \text{s}^{-1}$) [5]. However, the reported electron mobility of bulk ZnO is as high as $\sim 200\ \text{cm}^2\ \text{V}^{-1}\ \text{s}^{-1}$. Therefore, a further enhancement of the field-effect mobility of ZnO TFTs is possible. The channel current is $2.2 \times 10^{-9}\ \text{A}$ at a gate voltage of $0\ \text{V}$. The on/off current ratio is on the order of 10^4 at a gate voltage of $40\ \text{V}$ and a drain voltage of $10\ \text{V}$. Gate leakage current densities are $4 \times 10^{-7}\ \text{A}/\text{cm}^2$ at a bias of $10\ \text{V}$ (or under an electrical field of $0.5\ \text{MV}/\text{cm}$) and $6.4 \times 10^{-7}\ \text{A}/\text{cm}^2$ at a bias of $50\ \text{V}$ (or $2.5\ \text{MV}/\text{cm}$). However, these devices show a large flatband voltage and a large subthreshold swing, i.e., the variation in V_{GS} when I_{DS} decreases by one order of magnitude. The large subthreshold swing indicates the existence of a large interface state density. The possible reasons are that the purity of the ceramic ZnMgO targets used in these devices is low and the ion charge densities are possibly high. The reduction of the impurity density and enhancement of the crystalline quality of the H-ZnMgO and C-ZnMgO films are two critical issues to improve the quality of these new current devices in future work.

IV. CONCLUSION

We have demonstrated an enhancement-mode ZnMgO stack structure for TFTs. H-ZnMgO used as active channel and C-ZnMgO used as gate insulator for TFT devices were successively grown at low temperature in the same deposition chamber on patterned ITO-coated glass. The high- κ C-ZnMgO isolating layer shows leakage current characteristics of $4 \times 10^{-7}\ \text{A}/\text{cm}^2$ under an electrical field of $0.5\ \text{MV}/\text{cm}$ and $6.4 \times 10^{-7}\ \text{A}/\text{cm}^2$ under an electrical field of $2.5\ \text{MV}/\text{cm}$. C – V properties measured across the gate indicate that the H-ZnMgO channel is n-type. Enhancement-mode TFT devices are realized and display an on/off ratio on the order of 10^4 and a channel mobility of $1.5\ \text{cm}^2\ \text{V}^{-1}\ \text{s}^{-1}$. The ZnMgO TFTs fabricated at low growth temperature may be integrated with p-type ZnO materials [18] to fabricate ZnMgO-based optoelectronic devices on glass or flexible plastic substrate.

REFERENCES

- [1] Y. He, R. Hattori, and J. Kanicki, "Improved a-Si:H TFT pixel electrode circuits for active-matrix organic light emitting displays," *IEEE Trans. Electron Devices*, vol. 48, no. 7, pp. 1322–1325, Jul. 2001.
- [2] J. H. Kim, Y. Hong, and J. Kanicki, "Amorphous silicon TFT-based active-matrix organic polymer LEDs," *IEEE Electron Device Lett.*, vol. 24, no. 7, pp. 451–453, Jul. 2003.
- [3] C. Yoo, D. J. Kim, and K. L. Lee, "Threshold voltage and mobility mismatch compensated analogue buffer for driver-integrated poly-Si TFT LCDs," *Electron. Lett.*, vol. 41, no. 2, pp. 65–66, Jan. 2005.
- [4] H. Hara, M. Sakurai, M. Miyasaka, S. W. B. Tam, S. Inoue, and T. Shimoda, "Low temperature polycrystalline silicon TFT fingerprint sensor with integrated comparator circuit," in *Proc. 30th ESSCIRC*, 2004, pp. 403–406.
- [5] J. Nishii, F. M. Hossain, S. Takagi, T. Aita, K. Saikusa, Y. Ohmaki, I. Ohkubo, S. Kishimoto, A. Ohtomo, T. Fuhumura, F. Matsukura, Y. Ohno, H. Koinuma, H. Ohno, and M. Kawasaki, "High mobility thin film transistors with transparent ZnO channels," *Jpn. J. Appl. Phys.*, vol. 42, no. 4A, pp. L347–L349, Apr. 2003.
- [6] A. Ohtomo, M. Kawasaki, T. Koida, K. Masubuchi, H. Koinuma, Y. Sakurai, Y. Yoshida, T. Yasuda, and Y. Segawa, "Mg_xZn_{1-x}O as a II–VI widegap semiconductor alloy," *Appl. Phys. Lett.*, vol. 72, no. 19, pp. 2466–2468, May 1998.
- [7] P. Bhattacharya, R. R. Das, and R. S. Katiyar, "Fabrication of stable wide-band-gap ZnO/MgO multilayer thin films," *Appl. Phys. Lett.*, vol. 83, no. 10, pp. 2010–2012, Sep. 2003.
- [8] S. Masuda, K. Kitamura, Y. Okumura, and S. Miyatake, "Transparent thin film transistors using ZnO as an active channel layer and their electrical properties," *J. Appl. Phys.*, vol. 93, no. 3, pp. 1624–1630, Feb. 2003.
- [9] Y. Kwon, Y. Li, Y. W. Heo, M. Jones, P. H. Holloway, D. P. Norton, Z. V. Park, and S. Li, "Enhancement-mode thin-film field-effect transistor using phosphorus-doped (Zn,Mg)O channel," *Appl. Phys. Lett.*, vol. 84, no. 14, pp. 2685–2687, Apr. 2004.
- [10] R. L. Hoffman, B. J. Norris, and J. F. Wager, "ZnO-based transparent thin-film transistors," *Appl. Phys. Lett.*, vol. 82, no. 5, pp. 733–735, Feb. 2003.
- [11] K. Nomura, H. Ohta, A. Takagi, T. Kamiya, M. Hirano, and H. Hosono, "Room temperature fabrication of transparent flexible thin-film transistors using amorphous oxide semiconductors," *Nature*, vol. 432, no. 7016, pp. 488–492, Nov. 2004.
- [12] N. Chen, H. Wu, D. Qiu, T. Xu, J. Chen, and W. Shen, "Temperature dependent optical properties of hexagonal and cubic Mg_xZn_{1-x}O thin film alloys," *J. Phys.: Condens. Matter*, vol. 16, no. 17, pp. 2973–2980, May 2004.
- [13] J. Liang, H. Z. Wu, and Y. F. Lao, "Application of cubic MgZnO thin films in metal–insulator–silicon structure," *Chin. Phys. Lett.*, vol. 21, no. 6, pp. 1135–1138, Jun. 2004.
- [14] H. Z. Wu, K. M. He, D. J. Qiu, and D. M. Huang, "Low-temperature epitaxy of ZnO films on Si(001) and silica by reactive e-beam evaporation," *J. Cryst. Growth*, vol. 217, pp. 131–137, Jul. 2000.
- [15] S. Choopun, R. D. Vispute, W. Wang, R. P. Shama, T. Venkatesa, and H. Sen, "Realization of band gap above 5.0 eV in metastable cubic-phase Mg_xZn_{1-x}O alloy films," *Appl. Phys. Lett.*, vol. 80, no. 9, pp. 1529–1531, Mar. 2002.
- [16] N. B. Chen, H. Z. Wu, and T. N. Xu, "Refractive indices of cubic-phase Mg_xZn_{1-x}O thin-film alloys," *J. Appl. Phys.*, vol. 97, no. 2, pp. 23 515.1–23 515.4, Jan. 2005.
- [17] J. Liang, H. Z. Wu, N. B. Chen, and T. N. Xu, "Annealing effect on electrical properties of high-*k* MgZnO film on silicon," *Semicond. Sci. Technol.*, vol. 20, no. 5, pp. L15–L19, May 2005.
- [18] W. Z. Xu, Z. Z. Ye, Y. J. Zeng, and L. P. Zhu, "ZnO light-emitting diode grown by plasma-assisted metal organic chemical vapor deposition," *Appl. Phys. Lett.*, vol. 88, no. 17, pp. 173 506.1–173 506.3, Apr. 2006.



Huizhen Wu received the B.S. degree in physics from Hangzhou University, Hangzhou, China, in 1982 and the Ph.D. degree in semiconductor physics and electronics from the University of Manchester Institute of Science and Technology, Manchester, U.K., in 1995.

He joined Zhejiang University, Hangzhou, as a Lecturer in 1995 and has been a Faculty Member of the Department of Physics, where he is currently a Professor. In 1998, 2000, and 2001, he was a Visiting Fellow with the School of Electrical and Computer Engineering, University of Oklahoma, Norman. He has authored or coauthored more than 80 papers published in international journals and conference proceedings. He is the holder of more than ten patents. He is an Associate Editor of the *International Journal of Infrared and Millimeter Waves*. His research interests are semiconductor physics and devices.

Dr. Wu is a Committee Member of the China Society of Semiconductor Physics.

Jun Liang, photograph and biography not available at the time of publication.

Guofen Jin, photograph and biography not available at the time of publication.

Yanfeng Lao, photograph and biography not available at the time of publication.

Tianning Xu, photograph and biography not available at the time of publication.